Int. J. Electrochem. Sci., 13 **(2018)** 11702 – 11719, doi: 10.20964/2018.12.41

International Journal of
ELECTROCHEMICAL
SCIENCE
www.electrochemsci.org

Simultaneous determination of Dopamine, Uric acid and Folic acid with Electrochemical Techniques based on Co_3O_4/rGO/CTAB Modified Carbon Paste Electrode

M. Venu[1]*, Viond Kumar Gupta*[2,*]*, Shilpi Agarwa*[4]*, Sada Venkateswarlu*[3]*, G. Madhavi*[1,*]

[1] Electrochemical Research Laboratory, Department of Chemistry, Sri Venkateswara University, Tirupati, India,
[2] Department of Applied Chemistry, University of Johannesburg, South Africa.
[3] Department of Nanochemistry, Gachon University, Sungnam 13120, Republic of Korea
[4] King Abdulaziz University, Jeddah, Saudi Arabia
[*]E-mail: gmchem01@gmail.com, gmadhavi@svuniversity.edu.in. vinodfcy@gmail.com

Received: 14 August 2018 / *Accepted:* 17 October 2018 / *Published:* 5 November 2018

The electrochemical has been constructed based on Co_3O_4/rGO nanocomposite in presence of CTAB modified carbon paste electrode (CPE) and was developed for the simultaneous determination of dopamine, uric acid and folic acid at physiological pH 7.0 (PBS, 0.1 M). The physico-chemical analysis of nanocomposite was characterized by FT-IT, PXRD, SEM, TEM and EDX. The modified sensor showed well defined and stable reversible peak couple in both alkaline and aqueous solution. From the differential pulse voltammetry (DPV), the electrochemical sensor showed excellent electrocatalytic activity for the oxidation of dopamine, limit of detection (LOD) and limit of quantification (LOQ) of DA are calculated to be 2.8 µM and 10 µM, respectively. The Co_3O_4/rGO/CTAB MCPE showed an efficient electron mediating behavior with well defined oxidation peak potentials between DA to UA and UA to FA were 0.12 V and 0.39 V, respectively. From the cyclic voltammetry the results obtained for the linear calibration plots and the limit of detection of DA, UA and FA were calculated to be 7 µM, 94 µM and 19 µM, respectively. The developed sensor was successfully employed to sensing of DA in real samples.

Keywords: Cobalt Oxide; Cetyltrimethly Ammonium Bromide; Dopamine, Uric acid, Folic acid; Reduced graphene oxide; Cyclic Voltammetry; Differential Pulse Voltammetry

1. INTRODUCTION

Dopamine (3,4-dihydroxyphenethylamine) (DA) is a hormone and ubiquitous neurotransmitter in the mammalian due to its important physiological role in the central nervous system (CNS), cardiovascular and renal system [1, 2]. It is present on immune cells, especially lymphocytes is to reduce their activation levels [3]. Abnormal levels of DA will leads to neurological disorders such as Alzheimer's, Parkinsonism, Huntington's and Schizophrenia [4, 5] and to HIV infection [6]. Several technologies have been used to detect DA analysis such as spectrophotometry, flourometry, colorometry, chemiluminesence techquines, high-performance liquid chromatography (HPLC), electrophoresis and electrochemical techniques [7- 15].

Uric acid (2,6,8- trihydroxypurine) (UA) is major end product of purine metabolism in the human body and is excreted in the blood and urine [16]. The extreme abnormal level of UA will leads to several diseases such as hyperuricaemia, chronic renal and gout [17]. Until now, accurate determination of UA have been developed various analytical methods and procedures such as chemiluminicences, colorimetry, high-performance liquid chromatography (HPLC), amphorometric detection, biosensing and electrochemical methods [18- 25].

Folic acid (N-[p-[[(2-amino-4-hydroxy-t-tpiridinyl) methyl] amino]-benzoyl]-L-glutamic acid) (FA) is widely distributed vitamin (vitamin M, vitamin BC and vitamin B9) and it is an important component of the haematopoietic system. It can helps to fabricate healthy cells and is an potential agent for cancer prevention by anti oxidant activity [26]. The folic acid determination was required in clinical, pharmaceuticals, vegetable and food samples. Its biological significance comes from the reformation of tetrahydrofolate into dihydrofolic acid in the liver for the reason that electro activity of FA, several electrochemical methods has been worn for its determination of clinical, pharmaceuticals and food samples [27, 28].

The voltammetric simultaneous determination of DA in the presence of UA and FA owing to their great biological interest, playing a vital role in the human metabolism. Thus, the accuracy of the determination is extremely low in mixture mixture sample because of their coexistence in human fluids, it is very important to monitor their concentrations with more sensitive rapid and selective electrochemical sensors.

Past few decades, carbon based materials such as graphite, graphene and multi-walled carbon nanotubes has been employed for the development of various modified sensors [29- 31]. Among these, reduced graphene oxide has materialized as an superlative material for numerous applications such as electronic, energy and sensing, because of its remarkable optical, mechanical and electrochemical properties [31- 33]. Moreover, it has excellent electrochemical sensing because of its sp^2 hybridization, large surface area, ballistic conductivity and wide electrochemical potential window [34, 35]. Nowadays, the preparation of rGO has been used various kinds of reduction methods such as thermal, chemical and electrochemical.

Last few decades, several modified electrodes based on transition metal oxides, carbon based nanomaterials, higher metal ion based sensors, potentiometric sensors have An attracted considerable attention for electrochemical sensors applications [36- 43]. Among the different transition metals, cobalt oxide appeared as a shining star on the horizon of metal oxide catalyst due to its simple preparation procedures, various morphologies, excellent chemical durability [44]. Moreover, the cobalt oxide contains magnetic Co^{2+} distributed on tetrahedral sites and magnetic Co^{3+} on octahedral sites [45]. These polar sites of Co_3O_4 can play major role in the catalytic activity, especially facilitating rapid charge transfer kinetics on surface of the electrodes. Hence, various studies have reported cobalt oxide decorated on graphene oxide which has shown energy conversion, energy storage and electrochemical sensing applications [46- 50].

Surfactants can be widely used to modify the surface of the electrodes, such as carbon paste electrode (CPE) and glassy carbon paste electrode (GCE). Compared with other kind of electrodes, carbon paste electrode is more suitable, because the paraffin oil in the carbon paste gives a more hydrophobic surface which is in favor of the adsorption of surfactants on the electrode surface. Cetyltrimethylammonium bromide (CTAB) is a cationic surfactant and its non-polar chain interacts with the hydrophobic layer around the Co_3O_4, and as a result, the polar groups from CTAB are facing out, stabilizing the particles in the aqueous medium. Hence, we report the beneficial effect of CTAB with good sensitivity which facilitated their simultaneous determination in terms of peak separation of DA, UA and FA.

In this study, we introduced a simple synthetic method to prepare a cobalt oxide decorated reduced graphene oxide in the presence of CTAB. The fabricated Co_3O_4/rGO/CTAB composite was used to carbon paste electrode (CPE) and it was employed for investigation of electrochemical response was studied towards the detection of DA in the preseance of UA and FA at physiological pH 7.0 (PBS, 0.1 M). Furthermore, the developed electrochemical sensor can be employed to detection of DA real samples.

2. EXPERIMENTAL

2.1. Chemicals and reagents

Dopamine and Uric acid was obtained from Himedia Chemical Company. Folic acid purchased from Sisco Research Laboratories Pvt. Ltd., $CoCl_2$ $6H_2O$, CTAB, H_2O_2 (30%), H_2SO_4 were procured from Sigma-Aldrich, India. $KMnO_4$, $NaBH_4$, Na_2HPO_4, NaH2PO$_4$ were purchased from Merck, India. All aqueous solutions were prepared using double distilled water.

2.2 Instrumentation

The cyclic voltammetry and differential pulse voltammetry measurements were carried out with a CHI610D electrochemical analyzer operated by personal computer (Austin, USA.). a conventional three electrode cell was employed in the measurements, with the Co_3O_4/rGO/CTAB modified carbon paste electrode (3 mm, i.d.) as a working electrode, a Ag/AgCl (KCl, Sat.) as a reference electrode, a platinum wire (0.55 mm, CHI 115) as a counter electrode. The powder X-ray diffraction (PXRD) measurements were recorded using a Rigaku Ultima II X-ray diffractometer equipped with a Ni-filtered Cu-Kα radiation (λ = 1.54178 A^o), operated at 40 kV and 30 mA. Transmission electron microscopy (TEM, Tecnai G2) and a scanning electron microscope (SEM, S-4700, Hitachi, Japan) with an accelerating voltage of 20 kV was used for the analysis of structure and morphology of the Co3O4/rGO/CTAB. Energy dispersive X-ray spectroscopy (EDX) characterization was accomplished with a Hitachi SU900 microscope (Japan) was used for the analysis of composition.

The Fourier transform infrared spectroscopy (FT-IR) measurements were conducted between 500-4000 cm-1 at LASCO FTIR-4600 spectrometer.

2.3. Synthesis of graphene oxide

reduced graphene oxide (rGO) was prepared from a graphite powder by using a modified hummers methods with a small modification. Firstly, 3.0 g of graphite flaCkes of size ≤47 mM was added to the 100 mL of sulfuric acid in 500 mL of beaker continuously stirred in a ice bath of (0 ºC). Then, 12.0 g of potassium permanganate and 6.0 g of sodium nitrate were slowly added to the above mixture to keep the reaction temperature <10 ºC, the mixture was allow to stir for 4 h with temperature <10 ºC, and then allow to stir for 2 h at 35 ºC. After that 250 mL of deionized water was added to reaction mass. The mixture color turns to yellow. Later, the rGO suspension was washed with DI water and ethanol several times and the reaction mass was centrifuged at 5000 rpm with multiple times until the supernatant reaches the pH 7.0. the obtained rGO paste was dried under the oven for overnight at 70- 80 ºC to get rGO sheet.

2.4. Synthesis of Co_3O_4/rGO/CTAB nanocomposite

First, rGO was synthesized from graphite powder using the modified hummers method with a small modifications. Reduced graphene oxide (0.03 g) and CTAB (0.06 g) were dispersed into 50 mL of water followed by ultrasonic for 2 h. the suspension was let stand for 8 h and allows centrifuging the obtained GO/CTAB suspension at 5000 rpm. The precipitate was collected, washed plentifully with water several times and dispersed into 0.15 g of $CoCl_2$ $6H_2O$ in 60 mL of DI water under ultrasonic agitation for 30 min and subsequently adding 1 mL of NH_4OH. Finally, the light green suspension was poured into an 80 mL Teflon autoclave, and placed in a oven for 36 h at 80 ºC. The black product was collected by centrifugation, washed successfully with DI and ethanol then dried in a vacuum oven at 45 ºC for 8 h. Then, calcinations was carried out at 180 ºC for 4 h. Bare Co3O4 and Co_3O_4/rGO were also synthesized using same method, respectively.

2.5. Preparation of the electrode

The Co_3O_4/rGO/CTAB MCPE were prepared by mixing 0.168 g graphite powder, 0.072 g nanocomposite and 0.04 mL silicon oil with agate motor and paste thoroughly hand mixing to obtain a homogeneous carbon paste about 40 min. Later, the obtained modified carbon paste was packed into the cavity of end of the electrode with copper wire insert carbon paste provided an electrical contact (3 mm i.d. and 5 mm depth made in PVC rod on one side). When necessary, a shiny surface was obtained by pushing on excess of paste out of the tube, which was smoothly polished on the flat paper. Also, bare carbon paste electrode was prepared in the same manner but without adding nanocomposite to the mixture.

3. RESULT AND DISCUSSION

3.1. Characterization of the Co_3O_4/rGO/CTAB composite

TEM, SEM and EDX analyses were carry out to analysis the structure, morphology and composition of the synthesized Co_3O_4/rGO/CTAB composite.

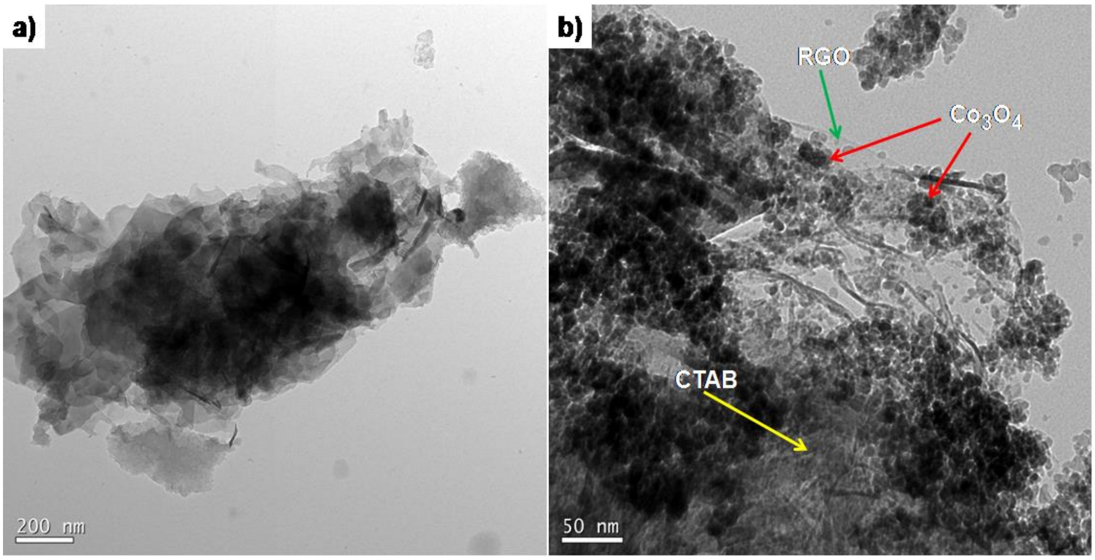

Figure 1. TEM images of GO (a) and Co_3O_4/rGO/CTAB (b) composite.

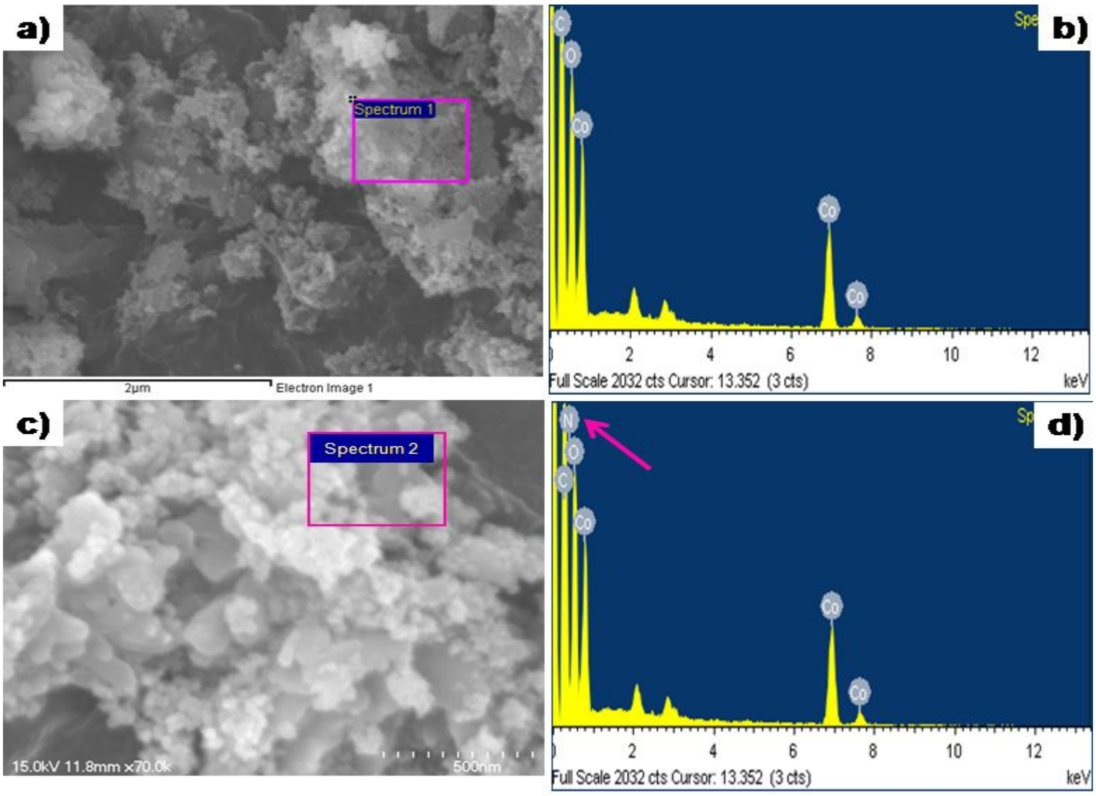

Figure 2. (a, b). SEM and EDX of Co_3O_4/rGO; (c, d). SEM and EDX of Co_3O_4/rGO/CTAB composite.

The TEM images of the bare GO and Co_3O_4/rGO/CTAB composite are shown in Fig. 1(a, b). The bare GO nanosheets are highly crumpled shown in Fig. 1(a). The spherical Co_3O_4 nanoparticles size nearly 12 nm (red arrow) are well embedded on the surface of the crumpled rGO (green arrow) and due to the presence of CTAB (yellow arrow) the Co_3O_4/rGO composite are slightly agglomerated shown in Fig. 1(b). Moreover, the morphology and composition was further confirmed by SEM, EDX analysis shown in Fig. 2(a-d). The EDX analysis Fig. 2(b) illustrates the presence of confirming the formation of Co_3O_4/rGO. Whereas, after addition of CTAB Fig. 2(d) shows, the presence of cobalt, oxygen, carbon and nitrogen elements which confirms the final Co_3O_4/rGO/CTAB composite.

PXRD were examined to analysis the phase purities of the as-synthesized GO and the Co_3O_4/rGO/CTAB composite. Fig. 3(a) illustrates a diffraction peaks at $2\theta = 19.0^{\circ}$, 31.2 º, 36.8 º 38.5 º, 44.8 º, 55.6 º, 59.3 º, 65.2 º, 68.6 º and 77.3 º corresponding to the planes of Co3O4 (111), (220), (311), (222), (400), (422), (511), (440), (531) and (533) respectively, which indexed the cubic phase Co_3O_4 coincide with the standard card (JCPDS card No. 49-1467) and no additional peak was observed, which illustrates the high purity of the material. Fig. 3(b) shows, the new peak at $2\theta = 22.6^{\circ}$ (002), indicating that presence of reduced GO along with the planes of Co_3O_4, which indicates the formation of Co_3O_4/rGO/CTAB composite. In addition, the particle size of the Co_3O_4 nanoparticles was calculated using the Debye-Scherrer equation ($D = 0.89\lambda/\beta\cos\theta$) according to diffraction peak of the (311) and the average particle size of Co_3O_4 is about 10 nm, which is very close to the TEM result. The above result confirms the formation of the Co_3O_4/rGO/CTAB composite.

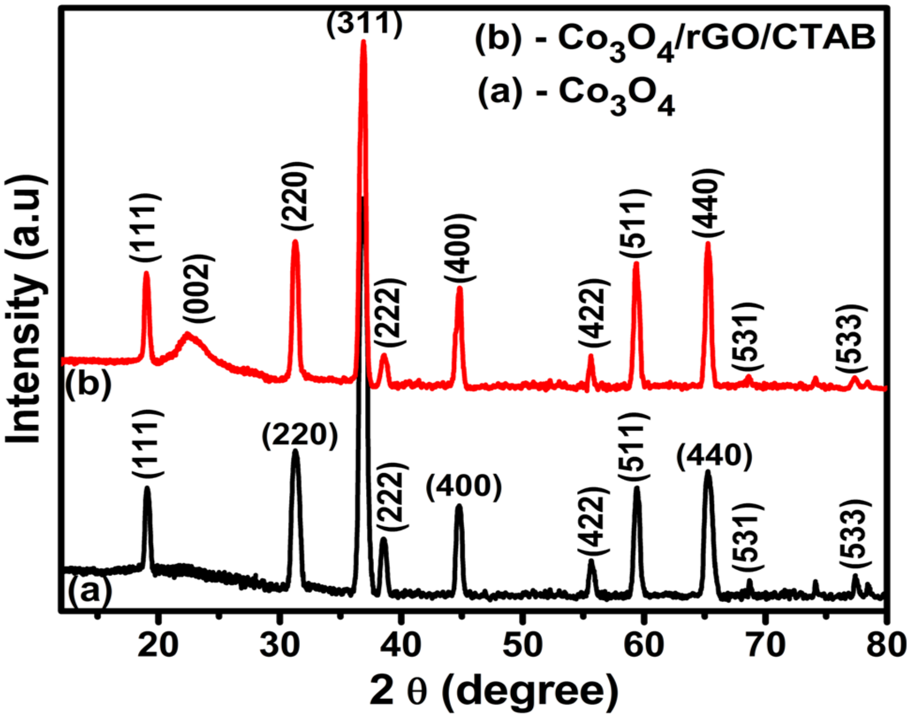

Figure 3. The PXRD pattern of the Co_3O_4 (a) and Co_3O_4/rGO/CTAB (b) composite.

The surface functional groups of GO and Co_3O_4/rGO/CTAB composite were analyzed by using FT-IR spectra at wave numbers of 400–4000 cm^{-1}. The bare GO has a large number of surface functional groups such as O–H, C-H, C=O, C=C, and C–O appeared the peaks at 3356, 2994, 2886, 1708, 1610, and 1037 cm^{-1}, respectively shown in Fig. 4(a). Whereas, the hydroxyl, carbonyl and epoxide functional groups had been disappeared and also overall peak intensities decrease significantly, which confirm reduction of pristine GO leads to the formation of rGO and also the peaks at 673 and 587 cm^{-1} indicates the presence of spinal Co_3O_4 shown in Fig. 4(b). The results confirm the formation of Co_3O_4/rGO/CTAB composite.

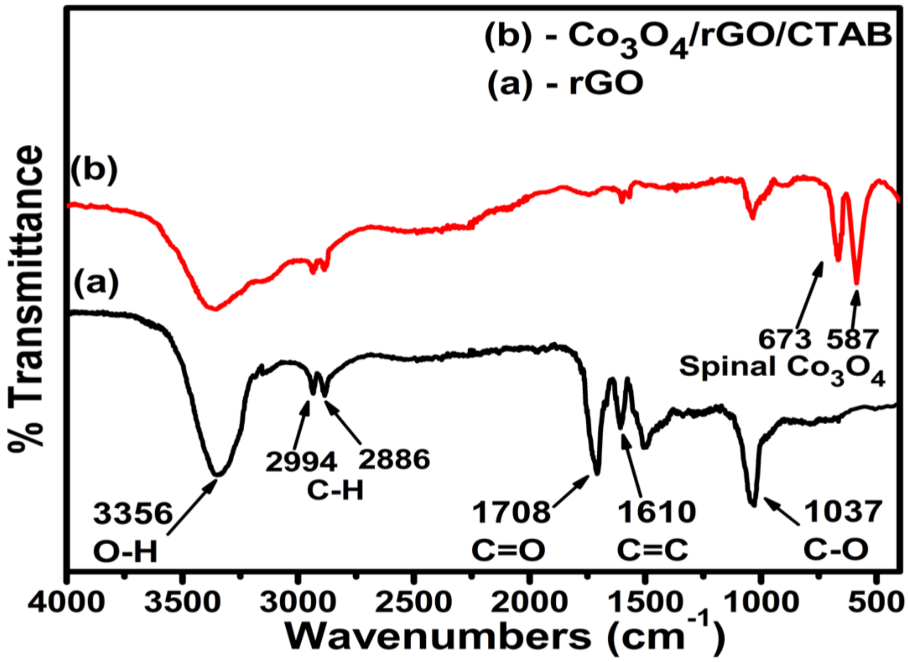

Figure 4. FTIR of rGO (a) and Co_3O_4/rGO/CTAB (b) composite.

3.2. Electrochemical behavior of DA on Co_3O_4/rGO/CTAB MCPE

The electrochemical oxidation current of DA on bare and modified carbon paste electrode was studied in PBS (0.1 M, pH 7.0) as a supporting electrolyte solution in presence of 1 mM of DA at 50mV.s-1 by using cyclic voltammetry. Fig. 5(a) shows, the cyclic voltammograms (CV) recorded on the bare CPE addition of 1 mM of DA to the supporting electrolyte solution results the anodic peak potential at E= 364 mV vs Ag/AgCl and cathodic peak potential observed at E= 279 mV vs Ag/AgCl is assigned to dopamine oxidation to dopaminequinone in the appearance of a reversible couple of peak. Fig. 5(b, c) shows, the cyclic voltammograms visualize the reversible peak current response of the Co_3O_4/rGO CPE and Co_3O_4/rGO/CTAB MCPE during the oxidation peaks of the same quantity of DA as that the bare CPE (1 mM of DA). Moreover, the high catalytic properties of cobalt on the modified Co_3O_4/rGO CPE causes about ~2-fold increases of the current in the redox peaks as compared to these recorded on the bare CPE shown in Fig. 5(b). However, the used modified electrode, the highest catalytic activity during the electrochemical oxidation of 1 mM of DA was attained on the Co_3O_4/rGO/CTAB MCPE shown in Fig. 5(c). In this case, the about 6-fold current peak response was observed during the electrochemical oxidation of DA. There is no doubt that the purpose for this highest electrocatalytic activity of the preceding electrode during the electrochemical oxidation of DA is synergistic result of the conducting material and changes in its magnetic, optical and electronic properties as compared to these characteristics for the metallic properties of cobalt. Finally, the obtained Co_3O_4/rGO/CTAB MCPE improves the characteristic of sensor to oxidize the DA.

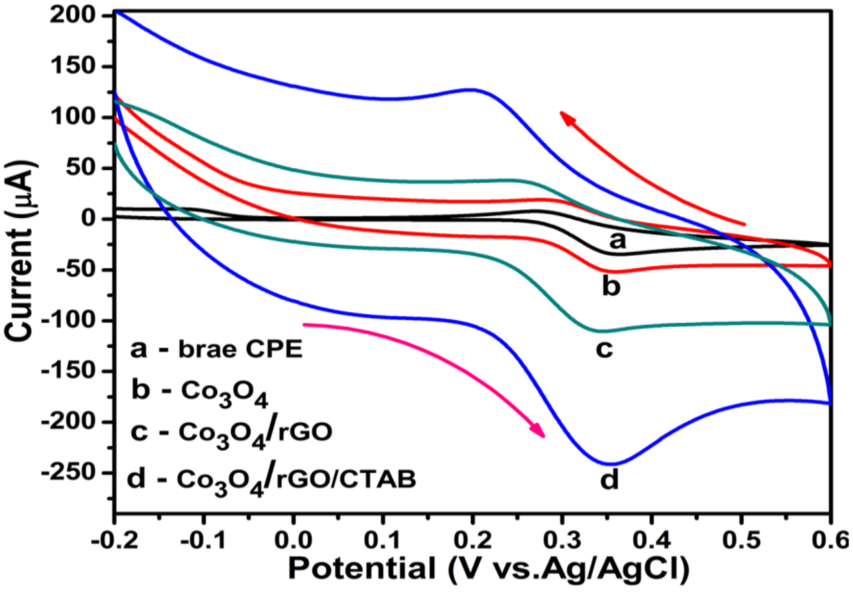

Figure 5. cyclic voltammograms recorded in PBS 0.1 M, pH 7.0 at the scan rate of 50 mV.s^{-1}.at (a) bare CPE, (b) Co_3O_4/CPE, (c) Co_3O_4/rGO/CPE and (d) Co_3O_4/rGO/CTAB/CPE modified electrode in the presence of 1 mM of DA.

3.3 effect of pH

The electrochemical determination of DA in the significant effect of various electrolyte pH on the Co_3O_4/rGO/CTAB was studied by effecting both current and potential. Fig. 6(a) shows, the obtained voltammograms, where the anodic peak current response of the 1 mM of DA increases from pH 5.5 to 7.0, until the value pH 7.0 is attained and then it is decreased from pH 7.0 to 8.0. For this reason the electrolytic solution chosen for the complete electrocatalytic studies. Fig. 6(b) shows, the graphical representation of the anodic peak current vs pH obtained from the cyclic voltammograms from which it is interfered that the maximum current peak was obtained at pH 7.0 and a higher value made the anodic potential to shift negatively for DA. The anodic potential shows, the linearity with the pH range of 5.5 to 8.0 and slope of the dEp/dpH being close to the theoretical value of 0.059 V/pH [51]. The linear regression equation is given

$$Epa(mV) = 0.057\frac{dEp}{dpH} + 0.8108\ (R^2 = 0.8582)$$

The slope value of 57 mV/pH showed that the same number of protons and electron are involved in the reaction [52, 53]. Therefore, to get high sensitivity and replicate the biological environment, Physiological pH 7.0 (PBS, 0.1 M) solution was used to study the other parameters.

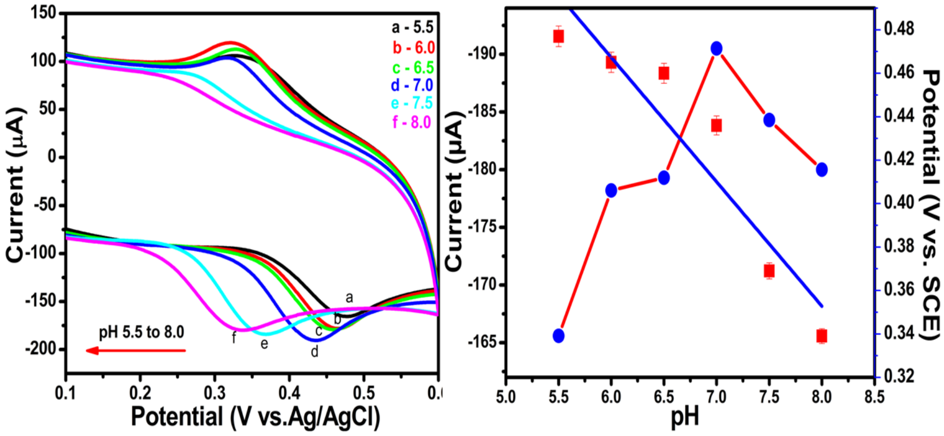

Figure 6. (a) CV voltammograms obtained at the Co_3O_4/rGO/CTAB/CPE electrode in electrolyte solution at different pH values with 1 mM DA. (b).Calibration plot of the anodic peak current (curve-I) and the anodic peak potential (curve-II) vs. pH of the 0.1 M PBS, pH 7.0 during electrooxidation of 1 mM DA at scan rate 50 mV.s^{-1}.

3.4. Effect of scan rate

Fig. 7(a) shows, the influence of electrocatalytic redox couple peak currents of 1 mM DA in the presence of supporting electrolyte solution pH 7.0 (PBS, 0.1 M) at Co_3O_4/rGO/CTAB MCPE by cyclic voltammetry was examined in the different sweep rates between 50-500 mV.s^{-1}. Fig. 7(b) shows, the linear relationship (R^2 = 0.9996 and 0.9986) between the anodic peak current and the scan rates clearly indicates that the electrochemical oxidation of DA on the Co_3O_4/rGO/CTAB MCPE is a diffusion controlled process [54]. Fig. 7(c) shows, a linear relationship between Ep values and the logarithmic of scan rates was obtained for determining the electro kinetic parameters of electrochemical reaction. The estimation of electrochemical parameters at different scan rates of DA was calculated by Laviron's equation.

$$E_{pa} = E^0 + \frac{2.3RT}{(1-\propto)nF}\log\vartheta$$

$$E_{pc} = E^0 - \frac{2.3RT}{\propto nF}\log\vartheta$$

Fig. 7(d) shows, a linear relationship obtained from the scan rates 250 mV to 500 mV. The calculated electron transfer coefficient (α) was 0.58 and the charge transfer coefficient k_s value was calculated by using the following Laviron's equation [55].

$$\log k_s = \propto \log(1-\propto) + (1-\propto)\log\propto - \log({}^{RT}/_{nF\vartheta}) \propto \frac{(1-\propto)nF\Delta E_p}{2.3RT}$$

Where, scan rate (υ), electron transfer coefficient (α), charge transfer rate constant (k_s), number of electron transferred (n), Farady constant (F), universal gas constant (R) and absolute temperature (T). the ks value was calculated to be 3.39 s^{-1}, representing that the electron transfer between the electrode and DA was enhanced by the addition of the Co_3O_4/rGO/CTAB MCPE.

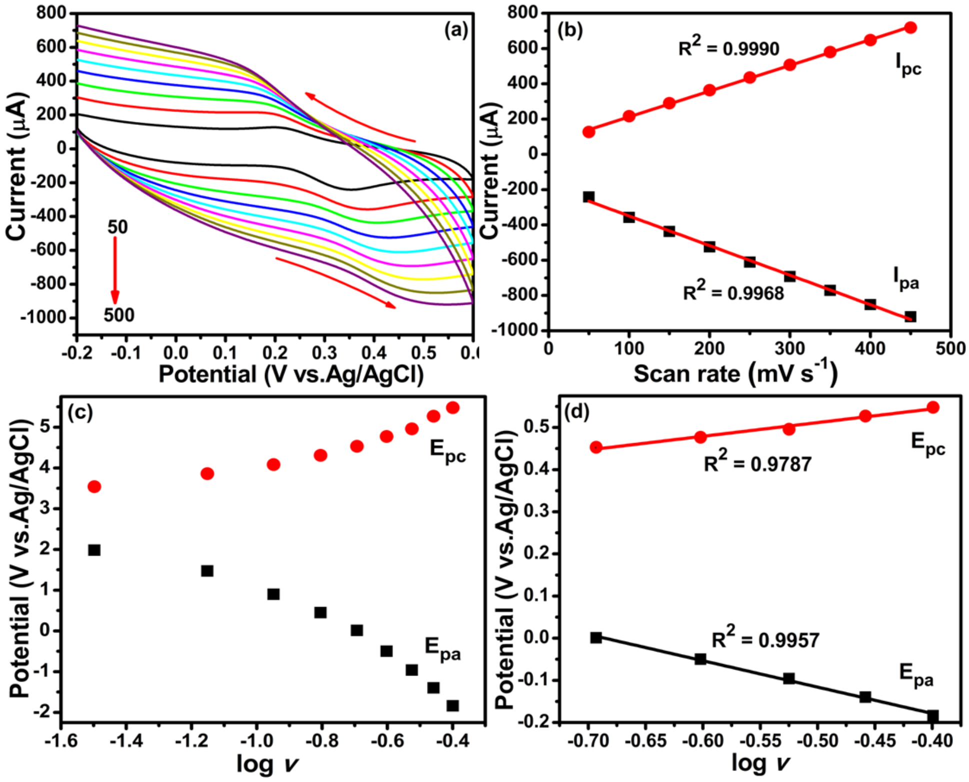

Figure 7. (a) CV recorded at the Co_3O_4/rGO/CTAB/CPE in presence of electrolyte solution at different scan rate from 50-500 mV.s^{-1}. (b). calibration plots of redox peak current vs. different scan rates from 50-500 mV.s^{-1}. (c). plot of variations in the redox peak potential values vs. log υ, with the scan rates from 50-500 mV.s^{-1}. (d). linear relationship between redox peak potential values and log υ with scan rates from 250-500 mV.s^{-1}.

3.5. Analytical performance of DA

Fig. 8(a) shows, to investigate the sensitivity response and to accomplish a lower detection limit was tested upon of the different DA concentrations on the Co_3O_4/rGO/CTAB MCPE in the linear dynamic range of 8.2-76 μM in the presence supporting electrolyte solution ph 7.0 (PBS, .01 M) by differential pulse voltammetry (DPV). Fig. 8(b) shows, the calibration plot between the anodic peaks current (Ipa) vs. concentrations of DA showing the linear dynamic range (LDR) from 8.2-76 μM in the supporting electrolyte solution at 50 mV.s^{-1}. The anodic peak current response was found to be in the entire LDR used with correlation coefficient 0.9992, and the detection of DA by using linear regression equation is expressed as

$$I_{pa}(\mu A) = 0.1098C\ \mu M/L + 98\mu A$$

Where, I_{pa} is the anodic peak current in μA. the concentration of DA is in μM. the limit of detection (LOD) and limit of quantification (LOQ) were estimated using the formulae [56, 57]

$$LOD = 3S/M$$

$$LOQ = 10S/M$$

Where, S is the standard deviation, M is the slope obtained from the calibration plots. From these data, the detection limit of DA was estimated to be 2.8 μM and the quantification limit is 10 μM.

the fabricated sensor is to be useful for real sample application. In addition, Table. 1 show, the detection of DA by using different electro analytical methods with limit of detection were compared with the developed sensor and anllytical data presented [50- 56].

Table 1. Caparison of limit of detection of DA with Co_3O_4/rGO/CTAB and various modified electrode

Electrode	Detection Limit (µM)	Method	Ref
Highly exposed (001) facets of titanium dioxide modified with reduced graphene oxide	6.0	DPV	50
Au-CA SAMS	2.3	DPV	51
Hydrogenated cylindrical carbon electrodes	7.5	CV	52
Metallothionenins self-assembled gold electrode	6.0	CV	53
Pd-NC/rGO/GCE	7.0	Amperometry	54
RGO-PAMAM-MWCNT-AuNP/GCE	3.3	DPV	55
Carbon paste-Modified GCE	1.5	DPV	56
Co_3O_4/rGO/CTAB CPE	2.8	DPV	This work

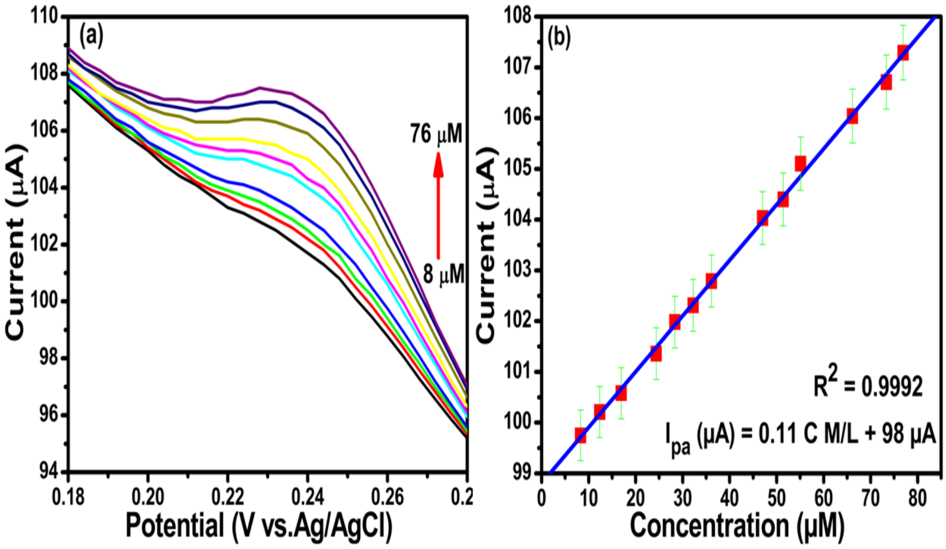

Figure 8. (a) DPVs recorded at the Co_3O_4/rGO/CTAB/CPE in the presence of DA over a concentration range 8.2-76 µM in pH 7.0 (PBS, 0.1 M). (b). the linear calibration plot of anodic peak current vs. DA concentrations.

3.6. Simultaneous and selective determination of DA, UA, and FA

The main object of this study, the electrochemical sensing of DA, UA, and FA simultaneously using the Co_3O_4/rGO/CTAB MCPE performed by cyclic voltammetry. The electrochemical sensing of

DA, UA, and FA cause problems using the bare electrodes suffers from the coexistence of DA, UA and FA owing to their almost similar oxidation potentials[56-84]. This was performed simultaneously changing their solution mixture containing 0.07-0.14 mM of DA, 0.7-1.46 mM of UA and 0.7-1.46 mM of FA, and increasing proportionally with the concentration and regarding the CV. Fig. 9(a) shows, the voltammetric results was observed that three well-prominent anodic oxidation peaks at potentials of 306, 428 and 819 mV, corresponding to the electrochemical oxidation of DA, UA and FA simultaneously without significance interference using Co_3O_4/rGO/CTAB. Fig. 9(b, c, d) shows, the linear relationship between the anodic peak current response and concentration of DA, UA and FA were observed with a correlation coefficient of 0.9899, 0.9854 and 0.9994 respectively, with the linear regression equation for DA, UA, and FA were expressed as $I_{pa}(\mu A) = 0.38C_{DA}\ \mu M/L + 86\mu A$, $I_{pa}(\mu A) = 0.043C_{UA}\ \mu M/L + 77\mu A$ and $I_{pa}(\mu A) = 0.056C_{FA}\ \mu M/L + 90\mu A$. The detection limit for the various concentrations of DA, UA, and FA were calculated as 7 μM, 94 μM and 19 μM with LDR from 0.07-1.46 mM.

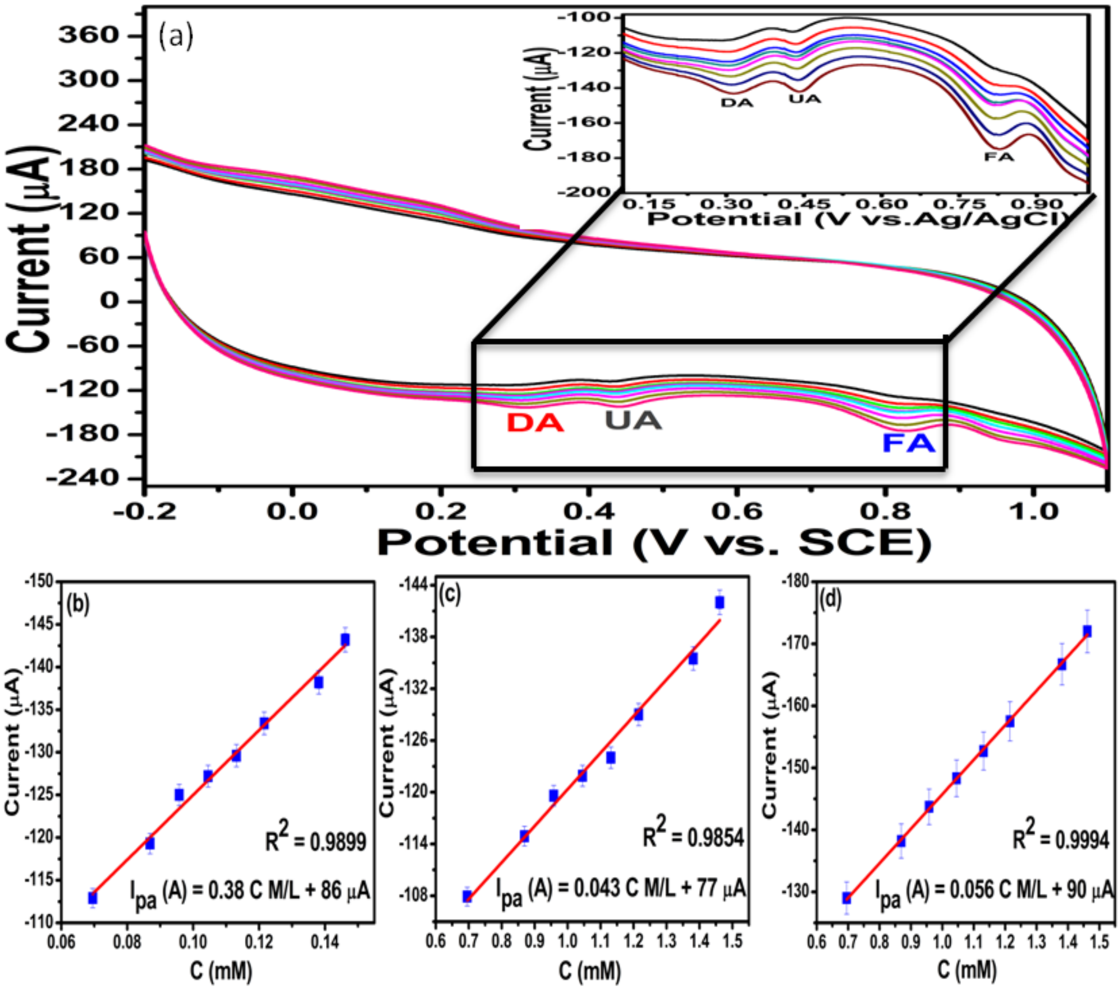

Figure 9. (a) CVs recorded on the Co_3O_4/rGO/CTAB/CPE modified electrode during simultaneous determination of 0.07-0.14 mM of DA and 0.7-1.46 mM of UA and 0.7-1.46 mM FA were prepared in 0.1 M PBS, pH 7.0. Fig. 9(b, c, d) The linear calibration plot anodic peak current versus the DA, UA, and FA concentrations

Fig. 10(a) shows, the DPV of the electrolyte solution mixture containing of DA was increased in the presence of 0.2 mM of UA, and 0.3 mM of FA were showed excellent sensitivity on the Co3O4/rGO/CTAB MCPE and there was no major change in the DA, UA and FA anodic peaks current. Fig. 10(b) shows, the linear relationship between the anodic peak current response and concentration of DA was observed with a correlation coefficient 0.9971, and the linear regression equation for DA is expressed as $I_{pa}(\mu A) = 0.0932C\ \mu M/L + 146\mu A$. Therefore, the detection limit for the various concentration of DA was calculated as 10.4 µM in the presence of UA and FA with the LDR from 40 to 220 µM.

Fig. 11(a) shows, the solution mixture containing the concentration of UA was increased in the presence of 0.05 mM of DA and 0.3 mM of FA. However, the electrochemical oxidation of anodic peak potential shifted to left when more UA concentration was added to the bio molecules. Fig. 11(b) shows, the calibration plot of anodic peak current and concentrations of UA was observed with a correlation coefficient 0.9897 and the linear regression equation $I_{pa}(\mu A) = 0.0161C_{UA}\ \mu M/L + 136\mu A$. Therefore, the detection limit for the various concentrations of UA was calculated as 63 µM in the presence of DA and FA with LDR from 50-108 µM.

In the similar way, FA concentration was increased in the presence of 0.06 mM of DA and 0.5 mM of UA shown in Fig. 12(a), Fig. 12(b) shows, the linear plot between the anodic peak current response and FA concentration was observed with a correlation coefficient of 0.9990, and the linear regression equation for FA is expressed as$(\mu A) = 0.0030C_{FA}\ \mu M/L + 132\mu A$. The detection limit for the various concentrations of FA was calculated as 95 µM in presence of DA and UA with LDR from 30-320 µM.

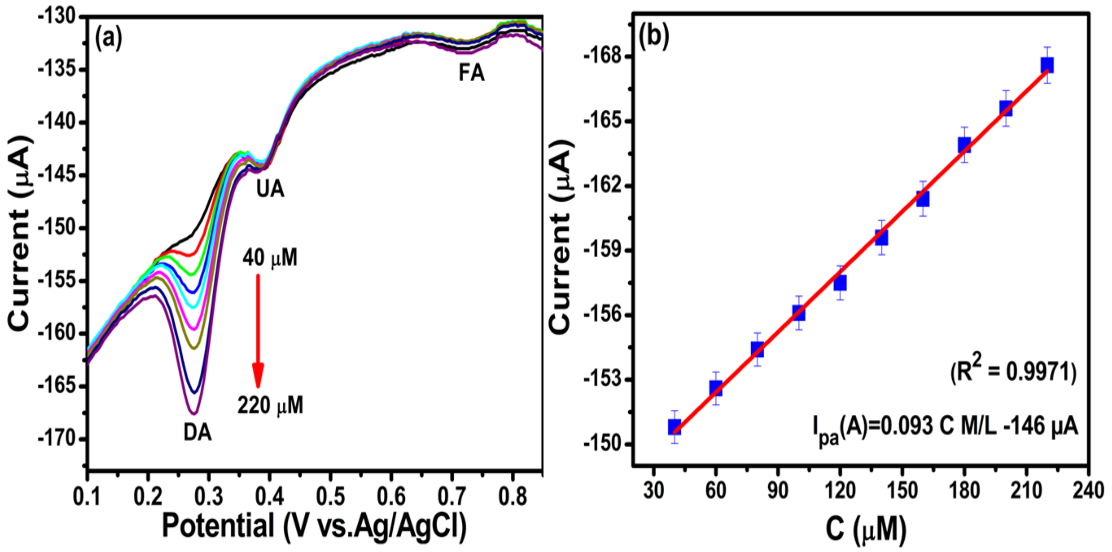

Figure 10. (a) DPV obtained for Co_3O_4/rGO/CTAB/CPE with 0.04-0.22 mM of DA in 0.1 MPBS (pH 7.0) in the preseance of 0.2 mM of UA, and 0.3 mM of FA. (b). The linear calibration plot anodic peak current versus the DA concentrations

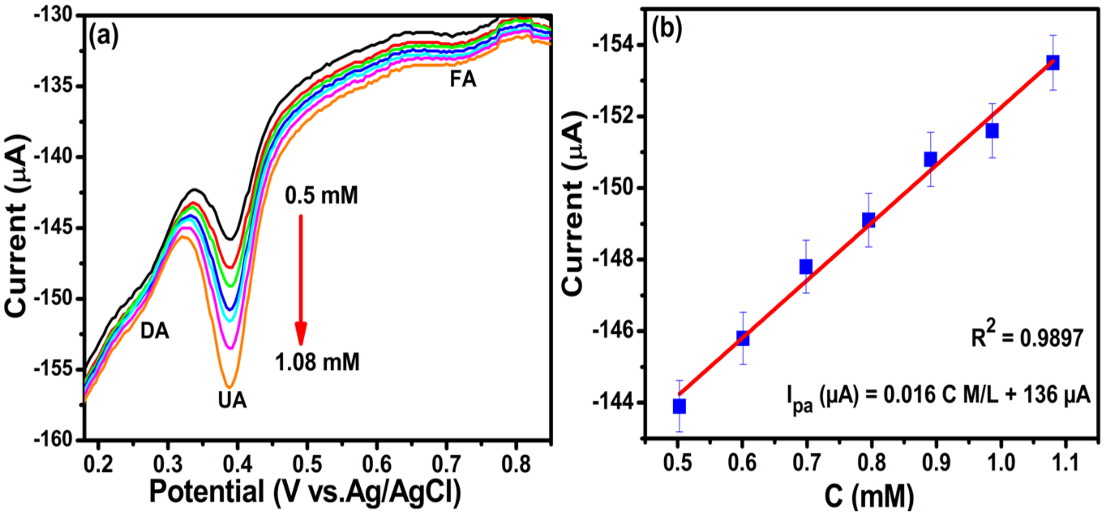

Figure 11. (a) DPV obtained for Co_3O_4/rGO/CTAB/CPE with 0.5-1.1 mM of UA in 0.1 MPBS (pH 7.0) in the preseance of 0.05 mM of DA, and 0.3 mM of FA. (b). the linear calibration plot anodic peak current versus the UA concentrations

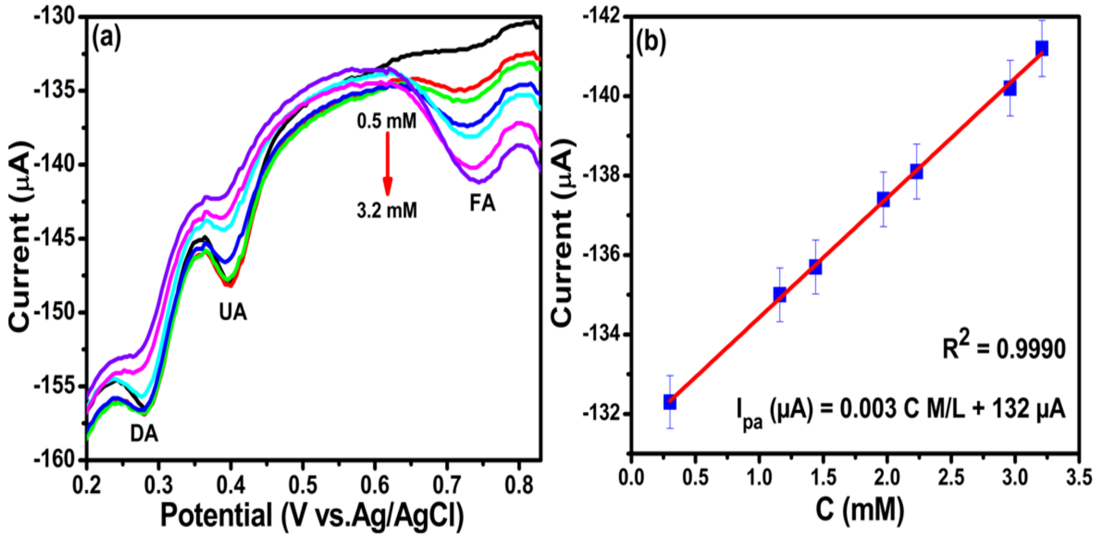

Figure 12. (a) DPV obtained for Co_3O_4/rGO/CTAB/CPE with 0.3-3.2 mM of FA in 0.1 MPBS (pH 7.0) in the presence of 0.06 mM of DA, and 0.5 mM of UA. (b). the linear calibration plot anodic peak current versus the FA concentrations

3.7. Analysis of DA in an injection sample and human serum

To estimate the applicability of the proposed technique, the Co_3O_4/rGO/CTAB MCPE was used for the electrocatalytic detection of a dopamine hydrochloride injection and human serum (From Health Centre of Sri Venkateswara University, Sri Venkateswara University, Tirupati, India.) were using the following method. 0.1 M of the human serum sample were diluted to 100 mL with pH 7.0 (PBS, 0.1 M) without any pretreatment and were used for further analysis. Each time 24 mL of this solution were added with various volumes of DA solutions of known concentrations to obtain various concentrations of spiked DA were analyzed by DPV.

The DA contains in the diluted injection samples (specified content of DA is 200 mg in 5 mL) was diluted to 25 mL with water, obtained various concentration of spiked DA levels were examined using the Co_3O_4/rGO/CTAB MCPE. The quantitative recovery of the obtained human serum and injection solution of DA were listed in Table. 2. Moreover, the results shows the proposed method for the determination of DA in human serum and injection samples were validated. Hence, the fabricated sensor was used for electro analytical applications in pharmaceutical industry and in the field of medicine for the diagnosis of DA deficiency.

Table 2. Determination of DA levels in injection sample and human blood serum using the Co_3O_4/rGO/CTAB MCPE.

Sample	Spiked (mM)	Found (mM)	Recovery (%)	RSD (%)
Drug injection	0.1	0.098	98.0	2.3
	0.2	0.211	105.5	4.8
	0.3	0.029	96.6	5.9
Human serum	0.1	0.109	109.0	6.5
	0.2	0.198	99.0	3.4
	0.3	0.311	103.6	5.8

4. CONCLUSION

In this work, we demonstrate the fabricated Co_3O_4/rGO/CTAB MCPE exhibited an excellent electrocatalytic activity with LDR from 8.2-76 µM and the detection limit of 2.8 µM towards the detection of DA by using DPV. The cyclic voltammetry technique was employed for the simultaneous determination of DA, UA and FA on the Co_3O_4/rGO/CTAB MCPE in presence of supporting electrolyte solution with the linear detection range 70-160 µM and the detection limits are 7 µM of DA , 94 µM of UA and 19 µM of FA. Hence, the Co_3O_4/rGO/CTAB MCPE is acts as an excellent electrochemical sensor for the determination of DA in the real samples.

CONFLICTS OF INTEREST

There are no conflicts of interest to declare.

ACKNOWLEDGEMENTS

Mr. Manthrapudi Venu is highly grateful to the UGC Letter No. F. 25-1/2013-14 (BSR)/7-187-2007 (BSR) dated: 19-11-2014. Government of India, New Delhi for providing financial assistance in the form of an award of meritorious fellowship (RFSMS).

References

1 P. Damier, E. C. Hirsch, Y. Agid and A. M. Graybiel, *Brain.*, 122 (1999) 1437.
2 O. Hornykiewicz, *Pharmacol. Rev.*, 18 (1966) 925.
3 F. R. Buttarelli, A. Fanciulli, C. Pellicano, F. E. Pontier, *Curr Neuropharmacol.*, 9 (2011) 278.
4 J. W. Mo, B. Ogorevc, *Anal. Chem.*, 73 (2001) 1196.
5 P. C. Pandey, A. K. Pandey, *Electrochim. Acta.*, 109 (2013) 536.
6 R. M. Wightman, L. J. May, A. C. Michael*, Anal Chem.*, 60 (1988) 769
7 A. N. Pham, T. D. Waite, *J. Inorg. Biochem.*, 137 (2014) 74.
8 C. Dı´az, C. Garcı´a, P. Iturriaga-Va´squez, M. J. Aguirre, J. P. Muena, R. Contreras, R. Ormaza´bal-Toledo, M. Isaacs, *Electrochim. Acta.*, 111 (2013) 846.
9 J. Li, B. M. Christensen, *J. Electroanal. Chem.*, 375 (1994) 219.
10 R. Cui, Y. Gu, L. Bao, J. Zhao, B. Qi, Z. Zhang, Z. Xie, D. Pang, *Anal. Chem.*, 84 (2012) 8932.
11 B. H. C. Westernik, J. Korf, *J. Neurochem.*, 29 (1977) 697.
12 Y. Lin, C. Chen, C. Wang, F. Pu, X. Qu, *Chem. Commun.*, (2011) 1181.
13 J. Kang, X. B. Yin, X. Yang, E. Wang, *Electrophoresis,* 26 (2005) 1732.
14 H. Tabel, M. Takahashi, S. Hoshino, O. Niwa, T. Horluchl, *Anal. Chem.*, 66 (1994) 3500.
15 X. P. Liu, J. Tong, Z. Yuan, Y. Yang, C. J. Mao, H. L. Niu, B. K. Jin, S. Y. Zhang, *J. Nanosci. Nanotechnol.,* 16 (2016) 1645.
16 E. Andreadou, C. Nikolaou, F. Gournaras, M. Rentzos, F. Boufidou, A. Tsoutsou, C. Zournas, V. Zissimopoulos, D. Vassilopoulos, *Clin. Neurol. Neurosurg.*, 111 (2009) 724.
17 T. Ghosh, P. Sarkar and A. P. F. Turner, *Bioelectrochemistry.*, 102 (2015) 1.
18 C. Vakh, S. Koronkiewicz, S. Kalinowski, L. Moskvin, *Talanta.*, 167 (2017) 725.
19 H. L. Feng, J. Y. Li, M. M. Zhang, Q. L. Zhang, *Sens. Actuators*, B., 244 (2017) 77.
20 R. Zuo, S. Zhou, Y. Zuo, Y. Deng, *Food Chem.*, 182 (2015) 242.
21 L. Sun, J. Liu, P. Zhang, Y. Meng, C. Liu, Y. Ma, Q. Xie, W. Meng, *J. Electroanal. Chem.*, 739 (2015) 187.
22 S. Menon, K. G. Kumar, *LWT–Food Sci. Technol.*, 86 (2017) 8.
23 A. Stoyanova, S. Ivanov, V. Tsakova, A. Bund, *Electrochim. Acta.*, 56 (2011) 3693.
24 N. Chauhan, C. S. Pundir, *Anal. Biochem.*, 413 (2011) 97.
25 W. C. Wu, H. W. Chang, Y. C. Tsai, *Chem. Commun.*, 47 (2011) 6458.
26 Y. I. Kim, *J. Nutr. Biochem.*, 10 (1999) 66.
27 B. B. Prasad, R. Madhuri, M. P. Tiwari, P. S. Sharma, *Sens. Actuators*, B., 146 (2010) 321.
28 P. Kalimuthu, S. Abraham John, *Biosens. Bioelectron.*, 24 (2009) 3575.
29 D. C. Marcano, D. V. Kosynkin, J. M. Berlin, A. Sinitskii, Z. Sun, A. Slesarev, L. B. Alemany, W. Lu, J. M. Tour, *ACS Nano.*, 4 (2010) 4806.
30 W. S. Hummers, R. E. Offeman, *Preparation of Graphitic Oxide*, (1958) p. 1339.
31 K. M. Hassan,T. J. Fahimeh, N. Atar, M. L. Yola, V. K. Gupta, A. A. Ensaf, *Ind. Eng. Chem. Res.*, 54 (2015) 3634.
32 M. M. Shahid, F. S. Omar, K. Ramesh, S. Ramesh, *Sensors and Actuators* B., 238 (2017) 1043.
33 M. M. Shahid, P. Rameshkumar, W. J. Basirunc, W. Upul, W. S. Chiu, P. S. Khiew, N. M. Huang, *Electrochimica Acta.*, 259 (2018) 606.
34 M. Hosseini, M. Aghazadeh, M. R. Ganjali, *New J. Chem.,* 41 (2017) 12678.
35 K. J. Huang, L. Wang, J. Li, Y. M. Liu, *Actuators B Chem.*, 178 (2013) 671.

36 H. Chang, H. Wu, *Energy Environ. Sci*., 6 (2013) 3483.
37 V. K. Gupta, M. R. Ganjali, P. Norouzi, H. Khani, A. Nayak, S. Agarwal, *Critical Reviews in Analytical Chemistry*, 41 (2011) 282.
38 V. K. Gupta, K. M. Hassan, R. Sadegh, *Int. J. Electrochem. Sci*., 10 (2015) 303.
39 S. K. Srivastava, V. K. Gupta, S. Jain, *Anal. Chem.,* 68 (1996) 1272.
40 A. Asfaram, M. Ghaedi, S. Agarwal, I. Tyagib, V. K. Gupta, *RSC Adv*., 5 (2105) 18438.
41 V. K. Gupta, A. Nayak, S. Agarwal, B. Singhal., *Combinatorial Chemistry & High Throughput Screening,* 14 (2011) 284.
42 S. K. Srivastava, V. K. Gupta , S. Jain, *Analyst*. 120 (1995) 495.
43 S. K. Srivastava, V. K. Gupta, M. K. Dwivedi, S. Jain, *Anal. Proc*., 32 (1995) 21.
44 M. Jafarian, M. G. Mahjani, H. Heli, H. K. F. Gobal, M. H. Hamedi, *Electrochem. Acta*., 48 (2003) 3423.
45 J. Chen, X. Wu, A. Selloni, *Phys. Rev. B*., 83 (2011) 245204
46 M. M. Shahid, A. Pandikumar, A. M. Golsheikh, N. M. Huang, H. N. Lim, *RSC Adv* 4 (2014) 62793.
47 A. Numan, N. Duraisamy, F. S. Omar, Y. Mahipal, K. Ramesh, S. Ramesh, *RSC Adv*., 6 (2016) 34894.
48 A. Numan, M. M. Shahid, F. S. Omar, K. Ramesh, S. Ramesh, *Sensors Actuators B Chem*., 238 (2017) 1043.
49 M.M. Shahid, P.R. Kumar, A. Pandikumar, H.N. Lim, Y.H. Ng, N.M. Huang, *J. Mater. Chem*. A., 3 (2015) 14458.
50 M. M. Shahid, A. Pandikumar, A. M. Golsheikh, N. M. Huang, H. N. Lim, *RSC Adv*., 4 (2014) 62793.
51 N. I. Kovtyukhova, P. J. Ollivier, B. R. Martin, T. E. Mallouk, S. A. Chizhik, E. V. Buzaneva, A. D. Gorchinskiy, *Chem. Mater*., 11 (1999) 771.
52 B. Gurzęda, T. Buchwald, M. Nocuń, A. Bąkowicz, P. Krawczyk, *RSC Adv.,* 7 (2017) 19904.
53 S. Antoniadou, A. Jannakoudakis, E. Theodoridou, *Synth Met*., 30, 1989, 295.
54 E. Laviron, *J. Electroanal. Chem*., 101 (1979) 19.
55 Y. Veera Manohara Reddy, V. Prabhakara Rao, A. Vijaya Bhaskar Reddy, M. Lavanya, M. Venu, M. Lavanya, G. Madhavi, *Mater. Sci. Eng*. C., 57 (2015) 378.
56 K. Mallikarjuna, Y. Veera Manohara Reddy, Bathinapatla Sravani, G Madhavi,*, Haekyoung Kim, shilipi Agarwal Vinod kumar Guptha, *Journal of Electroanalytical Chemistry* 822 (2018) 163–170.
57 Y.Veera Manohara Reddy, Bathinapatla Sravani, Shilpi Agarwal, Vinod kumar Guptha G.Madhavi1, *Journal of Electroanalytical Chemistry* 820 (2018) 168–175.
58 Y. Veera Manohara Reddy, Bathinapatla Sravani, Diana M. Fernandes, Ch. Madhuri, L. Subramanyam Sarma, G. Madhavi, *Colloids and Surfaces* A 546 (2018) 293–300.
59 Y. Veera Manohara Reddy, Bathinapatla Sravani, T. Łuczak, M. Osińska, Hussen Maseed, P. Ragavendra, L. Subramanyam Sarma, V. V. S. S.Srikanth, G. Madhavi* *New Journal of Chemistry* 42 (2018) 3137-3146.
60 S. Kiranmai, Y. Veera Manohara Reddy, M. Venu, Ch. Madhuri, K. Anitha, G. Madhavi and A. Varada Reddy, *Anal. Bioanal. Electrochem*., 9, (2017) 154-163.
61 R. K. Shervedani, M. Bagherzadeh, S. A. Mozaffari, *Sens. Actuators* B., 115 (2006) 614.
62 E. Laviron, *J. Electroanal. Chem*., 101 (1979) 19.
63 G. Z. Hu, D. P. Zhang,W. L. Wu, Z. S. Yang, *Colloids Surf. B: Biointerfaces*., 62 (2008) 199.
64 Q. Wang, N. Li, W. Wang, *Anal. Sci.,* 18 (2002) 635.
65 Y. S. Hsieh, B. D. Hong and C. L. Lee, *Microchim. Acta*., 183 (2016) 905.
66 S. Wang, W. Zhang, X. Zhong, Y. Chai, R. Yuan, Anal. Methods., DOI: 10.1039/c4ay02086c
67 X. Zhang, Y. Ch. Zhang, L. X. Ma, *Sens. Actuators* B., 227 (2016) 488.
68 Vinod kumar Gupta B.Sethi, R.A.Sharma, Arvind Bhartia, *Journal of Molecular Liquids*, 177, 2013, 114-118

69 Vinod K. Gupta , M. R. Ganjali , P. Norouzi , H. Khani , Arunima Nayak & Shilpi Agarwal *Critical Reviews in Analytical Chemistry*, 41 (2011)282-313.
70 Suresh K. Srivastava, Vinod K. Gupta and Suresh Jain , *Analys*t, 120(1995)495-498.
71 Suresh K. Srivastava, Vinod K. Gupta, Mithalesh K. Dwivedi and Suresh Jain, Analytical Proceedings including Analytical Communications 32, 21-23 (1995).
72 Vinod K. Gupta , M. R. Ganjali , P. Norouzi , H. Khani , Arunima Nayak & Shilpi Agarwal (2011), *Critical Reviews in Analytical Chemistry*, 41:4, 282-313, DOI: 10.1080/10408347.2011.589773
73 Vinod Kumar Gupta, Hassan Karimi-Maleh, Roya Sadegh, , *Int. J. Electrochem. Sci*., 10 (2015) 303 – 316.
74 Suresh K. Srivastava, Vinod K. Gupta, and Suresh Jain, *Anal. Chem*. 1996, 68, 1272-1275.
75 Arash Asfaram,a Mehrorang Ghaedi,a Shilpi Agarwal,b Inderjeet Tyagib and Vinod Kumar Gupta*, RSC Adv., 2015,5, 18438-18450.
76 Vinod K. Gupta, Arunima Nayak, Shilpi Agarwal, Barkha Singhal.Combinatorial Chemistry & High Throughput Screening, 14, 2011, 284-302, Suresh K. Srivastava, Vinod K. Gupta and Suresh Jain , Analyst, 1995,120, 495-498
77 Suresh K. Srivastava, Vinod K. Gupta, Mithalesh K. Dwivedi and Suresh Jain , *Anal. Proc*., 1995,32, 21-23
78 K. M. Hassan,T. J. Fahimeh, N. Atar, M. L. Yola, V. K. Gupta, A. A. Ensaf, *Ind. Eng. Chem. Res*., 54 (2015) 3634.
79 V. K. Gupta, M. Naveen, L. Kumawat, A. K. Singh, *Sensors & Actuators*: B. 207 (2015) 216-223.
80 M. Ghaedi, S. Hajjati, Z. Mahmudi, Arjun Maity, I. Tyagi, V. K. Gupta,. *Chemical Eng. J*., 268(2015) 28-37.
81 M. L. Yola, V. K. Gupta, Tanju Eren, A. E. Şen, N. Atar, *Electrochimica Acta*,120 (2014) 204–211.
82 D. Robati, B. Mirza, M. Rajabi, O.Moradi, I. Tyagi., S. Agarwal, V. K. Gupta, *Chem Eng J.* 284 (2016) 687–697.
83 H. Karimi-Maleh, F. Tahernejad-Javazmi, H. Beitollahi, N. Atar, M.L. Yola, V. K. Gupta, A. A. Ensafi, *Ind. Eng. Chem. Res*., 54 (14)(2015) 3634–3639.
84 R. Saravanan, E. Thirumal, V. K. Gupta, V. Narayanan and A. Stephen, *J. Mol. Liq.,* 177 (2013) 394-401.